Experimental Investigation of an Aluminium Fuelled Vacuum Arc Thruster

IEPC-2015-54／ISTS-2015-b-54

Presented at Joint Conference of 30th International Symposium on Space Technology and Science 34th International Electric Propulsion Conference and 6th Nano-satellite Symposium, Hyogo-Kobe, Japan July 4 – 10, 2015

J. Kolbeck[1], D. Lines[2], A. Knoll[3]
Surrey Space Centre, Guildford, Surrey, GU2 7XH, United Kingdom

Abstract: This paper presents recent experimental results of two vacuum arc thrusters currently under development within the Surrey Space Centre. The first device, a direct current powered continuous thrust design, was characterized using a pendulum type thrust balance up to powers of 1 kW using three different propellants: aluminum, magnesium, and zinc. It was found that the measured specific impulse was far lower than anticipated: 146 s for aluminium, 28.2 s for magnesium, and 4.5 s for zinc. The likely cause for the low specific impulse was the high background pressure of 5×10^{-2} Torr, and non-optimal anode and cathode geometry for these initial experiments. The second device, a low power pulsed mode vacuum arc thruster operating on aluminum propellant, is also under development. This paper presents preliminary electrical characteristics of the pulse forming network, the discharge voltage and current behavior as measured in vacuum. Direct thrust measurements of the pulsed mode device have not been carried out at this point. The peak discharge current and voltage for this design were measured at 10 A and 80 V, with a time average power consumption of 4.2 W firing at a 54 Hz frequency. The formation and propagation of the cathode spot in the pulsed mode device is also investigated using photo imagery of the discharge.

Nomenclature

δ	=	structural damping coefficient
j	=	electrical current density vector
B	=	magnetic field vector
$\dot{m}$	=	mass flow rate
I_{sp}	=	specific impulse
T	=	thrust
g	=	standard earth gravity

I. Introduction

Vacuum arcs, which are commonly known as cathodic arcs, are well known in the physical vapor deposition community[1]. Their relatively high ion energy, high ion density and high ionization degree makes them highly desirable for applications such as decorative coatings, as well as thin film deposition[2], and ion implantation[3]. Vacuum arcs have been considered for propulsion systems due to the aforementioned properties. Such thrusters are

[1] Visiting Researcher, Dept. of Aeronautical and Aerospace Eng., TU Berlin, jkolbeck@mailbox.tu-berlin.de
[2] MSc. Student, Department of Mechanical, Medical and Aerospace Engineering, dl00065@surrey.ac.uk
[3] Lecturer, Department of Electronic Engineering, a.knoll@surrey.ac.uk

called vacuum arc thrusters, or VAT for short. These have similar advantages to PPTs such as the use of solid propellants that do not require valves, tanks, pipes or mass flow controllers. Commonly, VATs are used in a pulsed regime rather than in a steady-state regime. We report the successful testing of a steady-state prototype as well as a pulsed VAT. Pulsed vacuum arc thrusters have been reported to produce high specific impulses of over 3000 seconds[4]. The research in the last years has been focused on reducing the size of these systems so that they can be used in cubesats. Thruster systems of less than 300 grams or less have been reported by M. Keidar et al. and J. Schein et al. amongst other teams[4,5]. Low mass VAT systems are considered to be viable thrusters for Cubesats and spacecraft with micropropulsion needs[6]. Notably, VATs have been selected for the UWE-4 picosatellite orbit control system[7]. The current vacuum arc thruster research at The University of Surrey (UoS) has been investigating the use of light metals with low cohesive energies such as aluminium, zinc, and magnesium as the cathode material. Experiments performed by Anders and Yushkov[8] showed that the ion velocity of aluminum ions is about 15.4 km/s in the absence of a B-field giving a kinetic energy of 33.1 eV. Magnesium shows even more promise when it comes to ion velocity and kinetic energy. The values for Mg are 19.8 km/s and 49.1 eV, respectively. Zinc is a much slower but heavier species; the average ion velocity is 10.3 km/s and has a kinetic energy of 35.7 eV. The research work has also been focused in overcoming some of the inherent design difficulties that arise in such systems, such as cathode feed systems, arc stability and triggering of the discharge.

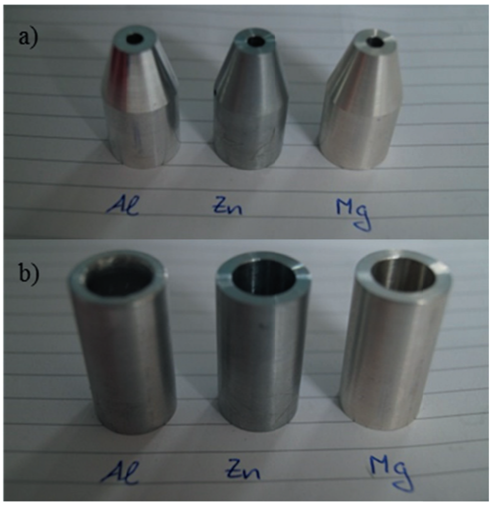

Figure 1. Cathode geometry used for the steady-state DC VAT. a) Cone-shaped cathodes. b) Tube-shaped cathodes. All cathodes were 35 mm high. The bottom diameter was 19 mm.

II. Vacuum Arc Thruster Design

This paper includes the findings from two systems designed at the UoS propulsion laboratory. The first thruster was designed to run on a steady-state DC mode for several seconds at a time. The second thruster was designed to run in a pulsed DC mode. The following subsections will deal with both designs in detail. The effect of using different gases and gas flow rates is subject of current investigation.

A. Steady-state DC Vacuum Arc Thruster

The steady-state DC VAT uses cathodes with a length of 35 mm and an outer diameter of 19 mm. For this thruster, two cathode geometries were used and analyzed. The first geometry consisted of cylindrical cathodes with a tapered end (cones), converging from 19 mm to 10 mm. The tapered section had a length of 15 mm. The second geometry was a hollowed-out cylinder (tubes). The cathode geometries can be seen in Fig. 1. Also, different cathode materials were tested, including aluminium, zinc and magnesium. The thruster was designed to run on a Sauvageau COLT 130G welding power supply unit (PSU). The PSU is capable of delivering up to 120 A. The maximum open circuit voltage was 69 V. To stabilize the discharge, an air-core inductor with an inductance of approximately 5.5 mH was used. The inductor was connected in series with a high power diode on the positive lead (anode potential) of the power supply. The tube-shaped anode of the thruster was machined out of brass and the cathode holder consisted of two parts that were united by a screw. This allowed mounting or removing of a permanent magnet ring. The shape of the cathode holder also allowed the permanent magnet to be moved closer or further away from the cathode. This was used to test different configurations in order to reach a stable arc discharge. The cathodes were held in place with the help of one set screw. This allowed for easy cathode exchange.

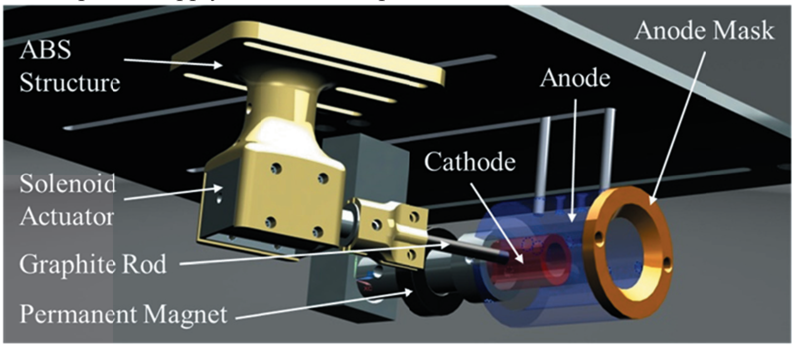

Figure 2. Rendered CAD model of the thruster apparatus mounted on the thruster bed.

1. Experimental (Thruster) Setup

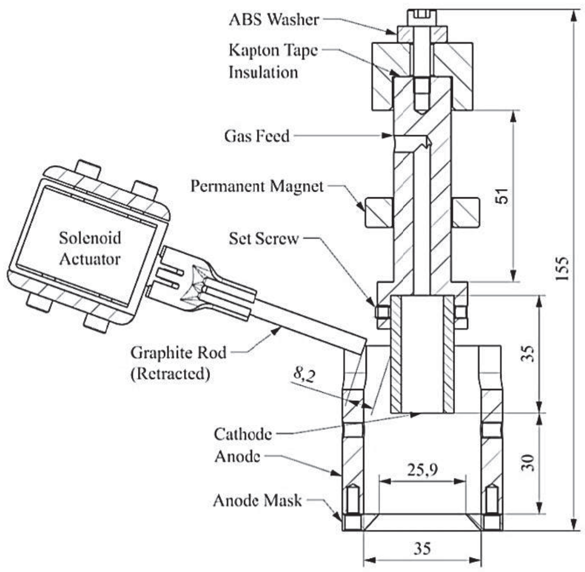

Figure 3. Cross-section of the steady-state VAT.

Figure 2 shows a rendered CAD model of the DC steady-state VAT. Figure 3 shows a cross-section of the VAT apparatus. The anode and the anode mask share the same potential with the graphite rod. The anode mask was designed to cover part of the plasma plume in order to measure the effect of the anode aperture on the plasma (thrust) output. The cathode, in this case a tube cathode, is shown in red. The magnetic field is created by the permanent magnet ring. The north pole of the magnet faced towards the cathode. The magnet produces a magnetic field in a through-field magnetic configuration on the cathode. This configuration was selected due to the acute angle rule (Robson angle) which causes the arc spot to be steered in the direction of the tangential component of the magnetic field relative to the cathode's surface's normal[1]. This effect is used in magnetically-steered arc sources to produce uniform cathode erosion[1]. In this arrangement, the preferred "burn" zone would be the top of the cathode. As can be seen from the CAD model, the thruster had no integrated cathode feed system. This proof-of-concept prototype did not require such a system. For space applications, it would be necessary to have means to feed the propellant as it is eroded (consumed).

The anode was suspended from a pendulum thrust balance by 2x 60 mm M4 threaded rods. In order to prevent the plasma from being ejected through the back side of the thruster, i.e. through the gap between the cathode holder and the anode, Kapton tape was used. While admittedly a placeholder for a ceramic part, the Kapton tape offered a quick way to make changes to the system's geometry and configuration. The tape was removed and replenished after each set of experiments. The rest of the components were also covered with this tape in order to increase the heat emissivity to provide a faster radiative cooling. Insulation between the thrust bed's aluminium plate and the thruster's threaded rods and screws was done with the use of ABS washers.

2. Trigger System and Discharge Initiation

The triggering system's structure consisted of two 3D-printed ABS components and can be seen in Fig. 4. One of them held a solenoid (pull) actuator with a stroke length of 10 mm in place. The holding force of the solenoid was 25 N. The second 3D printed component was attached to the actuator's shaft to isolate the solenoid actuator from the trigger. The trigger itself consisted of a graphite rod with a diameter of 5 mm and a length of about 50 mm. In its off-mode, the graphite rod held at anode potential was in direct electrical contact with the cathode inside the anode.

To ignite the discharge, current was passed in short circuit across the graphite rod. At this point, the actuator was activated and the force separated the graphite rod from the cathode, causing a voltage surge across the inductor which triggered an arc. The trigger worked reliably for over 140 discharges during these experiments.

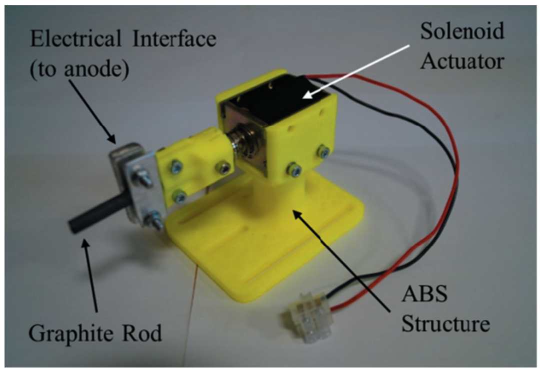

Figure 4. An image of the 3D printed holder for the solenoid actuator.

3. Experiment Settings and Metrology Setup

The experiments performed with this thruster were run at a current of 50 Ampere in intervals of 30 seconds with an off time of around 5 minutes to cool off the system. Thrust measurements were carried out inside a vacuum chamber with a volume of approximately 950 liters using only a mechanical backing pump at a rather high pressure of approximately 10^{-2} Torr. The thrust balance, an in-house design shown in Fig. 5, has an oscillation frequency of around 1.3 Hz with the thruster mounted on it. The structural damping coefficient was estimated to be $\delta \approx 0.03372\ 1/s$. Calibration was done using a 5 gram weight. The calibration coefficients were averaged between a total of 12 displacements (6 per direction). The average displacement per step was around 2.7 µm. Calibration of the thrust balance was performed each time a change in the setup was performed, e.g. when cathodes were replaced. The resulting calibration coefficients ranged from 0.19 N/mm to 0.23 N/mm. The displacements of the thrust balance were measured with a Micro-Epsilon optoNCDT 1700 laser interferometer at a rate of 312.5 Hz. The calibration and experiment data were analyzed with a Matlab script that uses the Butterworth low pass filter to filter out high frequency vibration modes. Fig. 6 shows an example of a calibration with 6 steps in each direction to test the linearity of the system, which resulted in a calibration constant of 0.20102 N/mm with an R^2 of 0.99981.

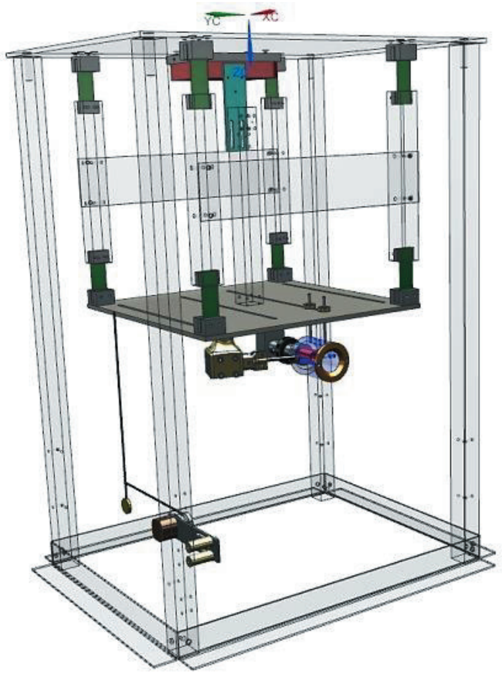

Figure 5. CAD model of the thrust balance with mounted thruster. The triangulation laser (red, top) is reflected by the laser target (turquoise, top) to measure the relative displacement caused by the produced thrust. The thin steel flextures (green) allow the displacement. The servomotor, the silk thread (black lines) and the calibration weight disc (5 grams) are shown in the bottom left corner.

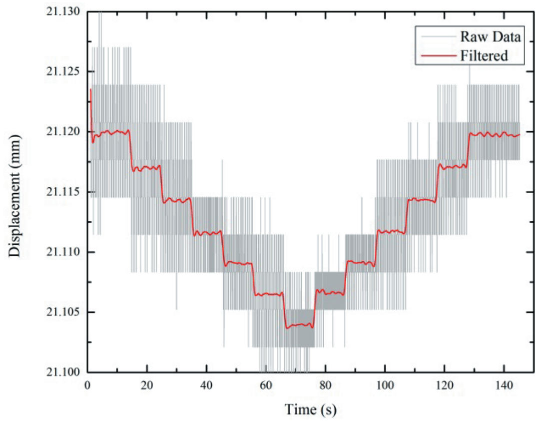

Figure 6. An example of filtered (red) and unfiltered (grey) calibration data. The calibration was done creating 6 displacements with a servo. For this example, the calibration constant was 0.20102 N/mm.

The measurement of the burning voltage was done with a digital multimeter attached between the anode and the cathode feed-throughs. High definition footage was acquired from different discharges with the use of a Canon XF105 video camcorder. Images of the discharge were taken with a Sony A37 DSLR camera at different shutter speeds.

Each experiment series was performed by using the following procedure: the discharge was started and was followed by a settling period of 20 seconds. After the 20 second mark was passed, the data acquisition program was started. At the 30 second mark, the thruster was turned off. This was followed by another settling period of a total of 15 seconds. This was done in order to make the on-off regimes clearly visible. The procedure was repeated 10 times for each series. After each series of experiments, the cathode was removed, weighed and a new cathode was installed in the thruster. Cathode weight measurements were taken using a Mettler Toledo B303-S precision scale. The setup was then calibrated and the experiment performed. The measured thrust data was filtered using the same filter as for the calibration data. The Matlab code created a linear approximation for the left and right sides of the thruster cutoff point. The difference in the y-values between these two linear functions at the cutoff point was correlated to the thrust using the calibration constant.

4. Preliminary Results

Thrust measurements were carried out using tube and cone-shaped cathodes (Fig. 1) for Al, Mg and Zn cathode materials. The first thrust measurements were made using the cathode-anode configuration shown in Fig. 2. In this arrangement, the distance between the exit plane and the front surface of the anode was approximately 30 mm. The aperture's cross-section was 5.27 cm^2. Removing the anode mask increased the total aperture cross-section by a factor of almost 1.83 to 9.62 cm^2.

Figure 7 shows the thrust distribution as a function of cathode material and cathode shape. An experiment series of 10 experiments was performed for each cathode material and shape except for the zinc tube. The cause was a cathode material failure after the fifth experiment. A fraction of the cathode melted and caused a direct short circuit between the cathode and the anode, thus stopping the plasma discharge. The cone-shaped zinc cathode showed no signs of melting.

The remaining part of the cathode was asymmetric; therefore, all further experiments with this cathode were cancelled. The zinc tube showed a high increase in thrust compared to the cone-shaped cathode. The most likely reason is that the higher temperature achieved during the discharges caused the production of neutral zinc atoms to be drastically increased due to the high vapor pressure of this material. Near the melting point of zinc at around 700 K, the vapor pressure of zinc is above 10^{-1} Torr. The drastic production of slow neutral particles has a severe negative effect on the specific impulse of the thruster and the overall durability of the cathode.

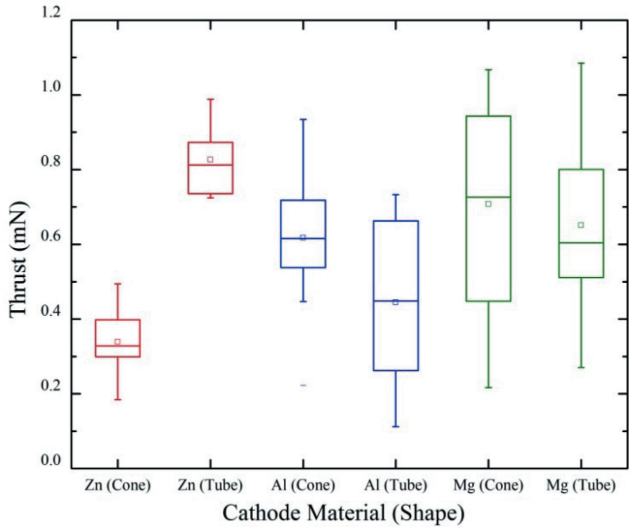

Figure 7. Thrust measurement distribution vs. cathode material and cathode shape. The mean value is described by the small square. The lone line in Al (cone) shows an outlier. Shown thrust measurements were taken with the anode mask.

The measured erosion rates can be read from Table 1. The highest thrust was produced by the magnesium cathodes likely owing to the high ion speed and relatively high material ablation rate. Aluminium produced a similar thrust to the magnesium cathodes but at a much lower total erosion rate.

Table 1. Cathode erosion rates $\dot{m}$ for each cathode material and cathode shape.

Cathode Material	Shape	Initial Mass [g]	Final Mass [g]	Discharge Time [s]	Erosion Rate [mg/s]
Zinc	Cone	54.789	49.430	300	17.86
Zinc	Tube	38.155	35.965	130	16.85
Magnesium	Cone	13.804	12.989	300	2.72
Magnesium	Tube	9.630	8.280	300	4.50
Aluminium	Cone	21.846	21.614	300	0.77
Aluminium	Tube	14.619	14.523	300	0.31

Using the average thrust values from Fig. 7 and the erosion rates from Table 1, one can approximate the specific impulse produced by the thruster. The calculation of the specific impulse I_{sp} can be calculated as follows:

$$I_{sp} = \frac{T}{\dot{m} \cdot g} \tag{1}$$

In this equation, T is the thrust, $\dot{m}$ the cathode erosion rate and g the standard earth gravity. The resulting specific impulses for the different cathodes and cathode shapes are shown in Table 2. These values were calculated by using the average thrust produced by each series. The mass flow rate was taken from Table 1.

Table 2: Specific impulse of the different cathode materials and shapes.

Zn (Cone)	Zn (Tube)	Mg (Cone)	Mg (Tube)	Al (Cone)	Al (Tube)
2 s	4.5 s	28.2 s	15.6 s	86 s	146 s

Figure 8 shows an image of the cathodes after the experiment series. The image was taken after all 6 cathodes had been used. The total erosion time can be read from Table 1.

Figure 8. Photo of the eroded cathodes after the 6 experiment series. The total erosion times can be found on Table 1. Noteworthy is the meltdown of the zinc tube cathode.

The differences plasma plumes produced by the three different cathode materials can be seen in Fig. 9. All three images were extracted from the video footage and have an exposure time of 1/29 seconds.

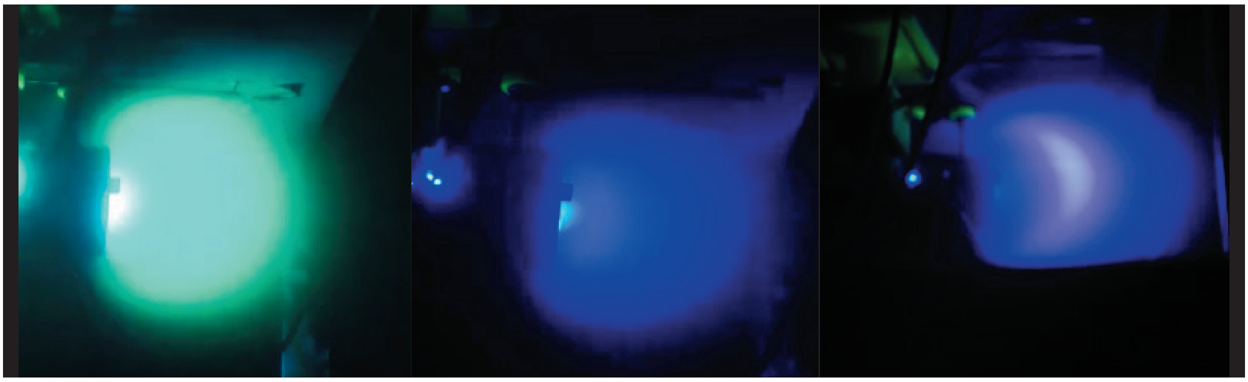

Figure 9. Discharge images taken with different cathodes. Left: magnesium, middle: aluminium, right: zinc. The images had an exposure time of 1/29 seconds.

The dynamics of the cathodic arc can be observed in Fig. 10. This figure captures the apparent motion of the cathodic arc spots. The human eye perceives what seems to be a continuous trace. In reality, the trace is actually a series of fast igniting and extinguishing cathode spots with a lifetime of only a few microseconds[1]. The images also show the retrograde "motion" of the arc spots in -j×B direction[9]. In this case and due to the magnetic field setup, this arc "motion" takes place in a clockwise manner. This can be seen clearly on the zinc and magnesium cathodes. The obvious change in color between the aluminium images in Fig. 9 and Fig. 10 is due to the severe oxidation of the cathode when the image on the latter figure was taken.

By looking at Fig. 10, one can notice the difference between the arc spots on a severely poisoned cathode (aluminium, type 1 spots) and on less strongly poisoned cathodes (magnesium and zinc, type 2 spots). Arc spots on a poisoned cathode are dim, small and mobile, whereas type 2 spots are brighter and slower[10]. All three images in Fig. 10 are snapshots of video footage and have the same exposure time of 1/29 seconds.

Changing the cathode configuration from the configuration without the anode mask to a position where the cathode and the anode were flush increased the thrust provided by the cone-shaped zinc cathode by a factor of approximately 2.8 to 2.49 mN. This is an increase of a factor of 6.9 compared to the thrust shown in Fig. 7. The highest thrust measured in this configuration with the zinc cathode was 3.3 mN. Experiments performed with the magnesium cathode corroborate this data. The produced thrust reached values of approximately 3.4 mN. It was expected that the Mg cathode would deliver a higher amount of thrust, as seen in Fig. 7. However, the discharge was fairly unstable and the arc spot did not burn in the proper position during the performed experiments.

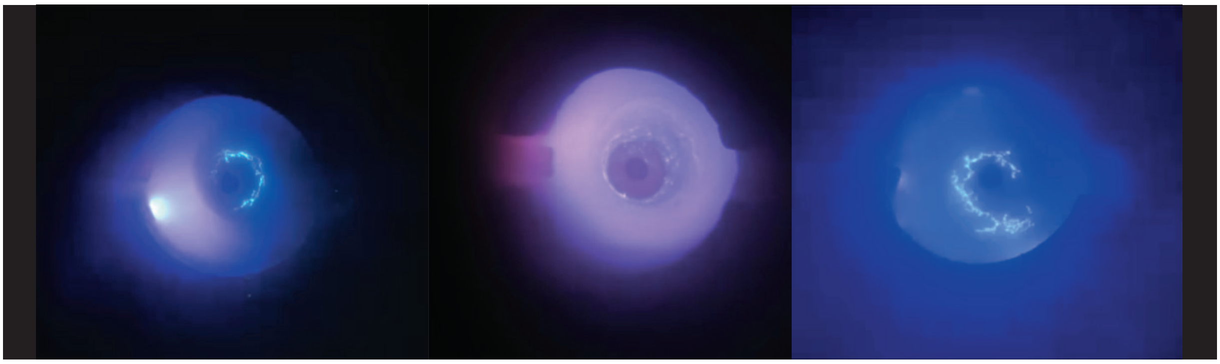

Figure 10. Photos of the discharges showing the apparent "motion" of the arc and its fractal nature. Left: magnesium, middle: aluminium, right: zinc. The arc spots move in a clockwise direction.

5. Sources of Error

The first source of error was oxidation of the aluminium cathode's surface, i.e. cathode poisoning. This was caused by the high pressure during the time of the experiments and was reflected in a white coloration of the cathode's surface (see Fig. 8). This assumption was confirmed after looking at the HD footage taken with the video recorder. The arc had switched from a metallic mode (type 2 spots) to a much faster arc mode (type 1 spots)[10]. The arc "speed" in poisoned aluminium cathodes can reach over 100 m/s compared to 15-20 m/s on clean aluminum cathodes as measured by J. Kolbeck and A. Anders[11]. The poisoning of the cathode also caused it to gain a few milligrams of mass. Aluminium oxide has a molecular mass of 101.96 g/mol whereas aluminium's molecular mass is 26.98 g/mol.

The second effect was caused by the continuously decreasing strength of the permanent magnet as the discharge counter increased. As previously mentioned, the thruster's body was not cooled. This caused all of the input power of around 1 kW to heat up the assembly. The heat could only be dissipated via radiation on most of the bodies and via thermal conduction on the attachment points. The radiative effect was greatly improved with the use of Kapton tape since it has a higher emission coefficient as aluminium. The conical magnesium cathode showed the same trend as the aluminium cathode.

B. Pulsed-Operation DC Vacuum Arc Thruster

The pulsed VAT is shown in Fig. 11. The thruster head had a total weight of approximately 84 grams including the permanent magnets. Its intended application is the use in small satellites, such as cubesats. The cathode material chosen for this system was aluminum due to its light weight, high ion velocity and low cost. Another chosen criterion was the low cohesive energy of this element (3.39 eV per atom).

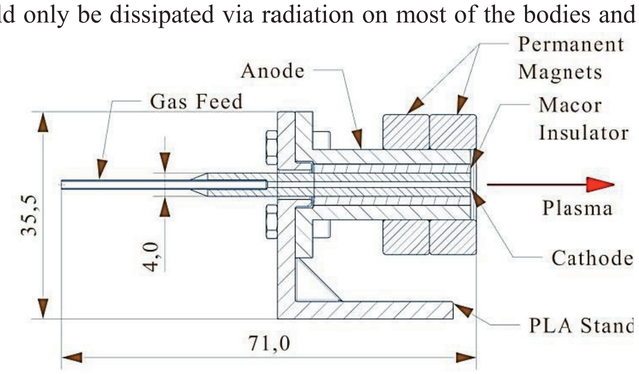

Figure 11. Pulsed VAT thruster. Dimensions in mm.

1. Experimental (Thruster) Setup

This system uses a concentric electrode configuration, as suggested by J. Polk's paper[12]. With this setup it is possible to achieve a high plasma output with axial-directed momentum. Therefore, this was the chosen configuration. In the center, the perforated cathode was surrounded by a Macor tube as an insulator. The anode was located concentrically around the ceramic. The thruster was designed in such a way as to allow gas to flow through the middle of the cathode. The effect of using different gases and flow rates is subject of current investigation.

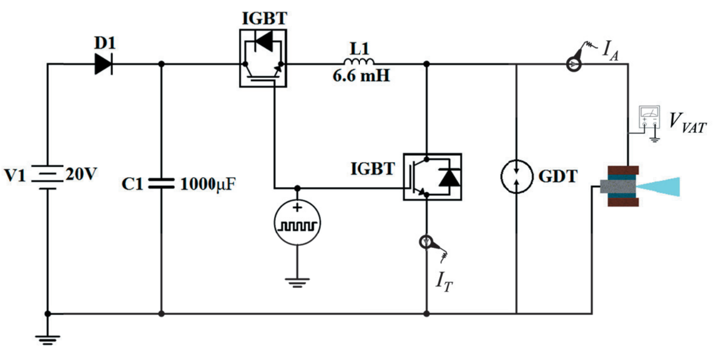

Figure 12. Pulse-forming network utilized for the pulsed vacuum

2. Trigger System and Discharge Initiation

Figure 12 shows the pulse-forming network (PFN) that was utilized for these experiments. Initially, the IGBT gates are closed allowing the capacitor C1 to charge. Next, both IGBTs open to allow current to flow from the capacitor to the inductor L1, which is shorted to ground. When the current passing through the inductor reaches its maximum level, the IGBTs are closed to force the current to pass through the cathode and the anode connected by a thin graphite layer[5,13] (~2.5 kΩ). The high voltage spike ionizes the surface of the graphite, causing the production of electrons and ions. These provide a conductive plasma path and "short circuit" the cathode and the anode, triggering the pulsed arc discharge and allowing the current to flow. The input voltage was 20 volts at a pulse-rate of 20 to 54 Hz. The PFN was able to produce a voltage spike of nearly 1.5 kV, although only 80 V were normally required to ignite the arc. The current spike produced by the PFN reached 10 amperes during the discharges.

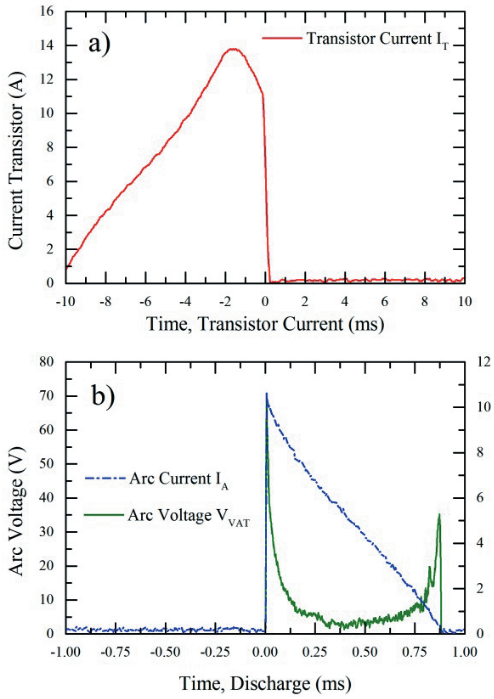

Figure 13. Circuit responses. a) Transistor Current, b) Arc Discharge.

3. Experiment Settings and Metrology Setup

The pulsed VAT was placed inside a vacuum chamber with a volume of 5500 liters. The base pressure of this system reaches the 10^{-6} Torr range with the help of a turbomolecular pump and a cryogenic pump. The parameters measured during the discharges included the arc voltage V_{VAT}, the arc current I_A and the transistor's current I_T. The location of the respective probes can be seen in Fig. 12. The signal response of the circuit has been recorded and is shown in Fig. 13. It is worth mentioning that both processes, the charging of the inductor L1 with I_T (Fig. 13, a)) and the actual arc discharge (Fig. 13, b)), occur on different time scales. Noteworthy is the fact that the arc discharge did not occur when the transistor current had reached its peak, but after. Triggering of the discharge at the peak of the transistor's current caused a sudden increase in the noise of the measured arc current, to the point that it was not possible to discern signal from noise. The cause for this disturbance is currently being investigated.

4. Preliminary Results

Figure 14 shows an image of the discharge of the pulsed VAT. The shutter speed was 1/160 seconds. Using the image processing program ImageJ and the shutter speed, the velocity of the arc trace was estimated to be approximately 1.25 meters per second. The arc trace seen on the image has a total distance of nearly 8 mm.

III. Conclusion

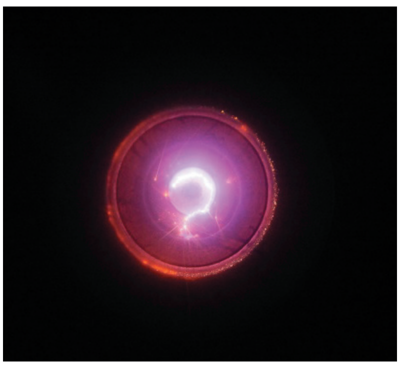

Figure 14. Image of the arc discharge's trace on the cathode's surface.

It is clear from the measurements gathered in this study that the DC powered steady-state VAT is performing far lower than expectations, reaching a maximum specific impulse of only 146 s using aluminium propellant. Theoretical predictions by Polk[12] suggest a specific impulse of over 1000 s for aluminium and magnesium. It is likely that the high background pressure (5×10^{-2} Torr) and non-optimal anode and cathode geometry were contributing factors. A revised test campaign at lower pressures ($< 1 \times 10^{-5}$ Torr) and a design with better anode and cathode geometry is the subject of future work. One of the main challenges with the steady-state VAT was the triggering of the discharge. For the laboratory experiments, the mechanical contact trigger offered a sufficient efficiency and reliability, but this kind of mechanical triggering mechanism is undesirable for space applications. Another design challenge for VATs is the feeding of the cathode material, regardless of whether they work in a pulsed or steady-state regime. This issue was not dealt with during this project but it will be necessary to deal with it should this technology become interesting for space applications. An improved magnetic field configuration may also contribute positively and improve the thrust. More testing will have to be done with a new power supply that can sustain a higher voltage, which would allow testing of materials with higher cohesive energies such as yttrium, chromium and tungsten.

Direct thrust measurements of the pulsed mode device require a specialized thrust balance, such as the one presented by J. Ziemer at the IEPC 2001[14], and have not been performed at this point. Current investigations have so far been limited to electrical measurements of the plasma arc discharge event. The peak discharge current and voltage for this design were measured at 10 A and 80 V, with a time average power consumption of 4.2 W firing at a 54 Hz frequency. Future work will be aimed at characterizing the properties of the plume in terms of the ion energy distribution, number density, and beam current as a function of cone angle.

Acknowledgments

The authors would like to thank Dr. André Anders from the Lawrence Berkeley National Laboratory for the discussions and insight provided regarding cathodic arcs. This research has been funded through the University of Surrey's strategic partnership with Airbus Defence and Space.

References

[1]Anders, A. Cathodic Arcs: From Fractal Spots to Energetic Condensation. Springer Science & Business Media, 2009.

[2]Mattox, D. M. Handbook of Physical Vapor Deposition (PVD) Processing. William Andrew, 2010.

[3]Bilek, M. M. M., et al. "Plasma-Based Ion Implantation Utilising a Cathodic Arc Plasma." Surface And Coatings Technology 156.1 (2002): 136-142.

[4]Keidar, M., et al. "Electric Propulsion for Small Satellites." Plasma Physics and Controlled Fusion 57.1 (2015): 014005.

[5]Schein, J., et al. "Low Mass Vacuum Arc Thruster System for Station Keeping Missions." IEPC Paper (2001): 01-228.

[6]Wright, W. P., And P. Ferrer. "Electric Micropropulsion Systems." Progress in Aerospace Sciences (2014).

[7]Kronhaus, I., et al. "Design of The UWE-4 Picosatellite Orbit Control System Using Vacuum-Arc-Thrusters." Proceedings of the 33rd International Electric Propulsion Conference. 2013.

[8]Anders, A., Yushkov, G. Y. "Ion Flux from Vacuum Arc Cathode Spots in the Absence and Presence Of A Magnetic Field." Journal Of Applied Physics 91.8 (2002): 4824-4832.

[9]Jüttner, B., Kleberg, I. "Retrograde Arc Spot Motion in Vacuum." Discharges and Electrical Insulation in Vacuum, 2000. Proceedings. ISDEIV. Xixth International Symposium on. Vol. 1. IEEE, 2000.

[10]Jakubka, K., Jüttner, B. "On the Influence of Surface Conditions on Initiation and Spot Types of Unipolar Arcs in a Tokamak." Journal Of Nuclear Materials 102.3 (1981): 259-266.

[11] Kolbeck, J.; Anders, A., "Unusual Cathode Erosion Patterns Observed for Steered Arc Sources," Plasma Science, IEEE Transactions on, Vol.42, No.10, Pp.2602,2603, Oct. 2014

[12] Polk, J. E.; Sekerak, M.J.; Ziemer, J.K.; Schein, J.; Qi, N.; Anders, A., "A Theoretical Analysis of Vacuum Arc Thruster and Vacuum Arc Ion Thruster Performance," Plasma Science, IEEE Transactions On , Vol.36, No.5, Pp.2167,2179, Oct. 2008

[13]Anders, A., et al. "Triggerless' Triggering of Vacuum Arcs." Journal Of Physics D: Applied Physics 31.5 (1998): 584.

[14]Ziemer, J. K. "Performance Measurements Using a Sub-Micronewton Resolution Thrust Stand." International Electric Propulsion Conference, IEPC-01-238, Pasadena. 2001.